J. Biochem. **133**, 343–349 (2003)
DOI: 10.1093/jb/mvg046

Anomalous Excitonic CD of *Meso*-Tetrakis(3-*N*-Methylpyridiniumyl)porphyrin Bound to Poly[d(A-T)$_2$]

Young-Ae Lee[1], Soomin Lee[1], Hyun Mee Lee[1], Chong-Soon Lee[2] and Seog K. Kim[*,1]

[1]Department of Chemistry and [2]Department of Biochemistry, Yeungnam University, 214-1 Dae-dong, Kyoungsan City, Kyoung-buk, 712-749 Republic of Korea

Received September 30, 2002; accepted January 6, 2003

When *meso*-tetrakis(3-*N*-methylpyridiniumyl)porphyrin (*m*-TMPyP) formed a complex with poly[d(A-T)$_2$], an intense bisignate excitonic CD in the Soret absorption region was observed. The excitonic CD of the *m*-TMPyP-poly[d(A-T)$_2$] complex is unique in that no other combination of the related porphyrin, namely, *meso*-tetrakis(*n*-*N*-methylpyridiniumyl)porphyrin (where *n* = 2, 4), and polynucleotide including calf thymus DNA, poly[d(G-C)$_2$], poly[d(I-C)$_2$], and poly(dA)·poly(dT), exhibits a comparable CD spectrum. From the [drug]/[DNA] ratio–dependence of the intensity and the shape of the CD spectrum, this porphyrin species is assigned to an extensively aggregated form. The extensively aggregated porphyrin disperses in 1 h after mixing to form moderately stacked porphyrin at a low mixing ratio. The magnitude of linear dichroism of the extensively aggregated porphyrin was small and the sign was negative in the Soret band, which indicated that the molecular plane of porphyrin in the complex is strongly tilted. On the other hand, the molecular plane of porphyrin is almost parallel to the DNA base plane (perpendicular to the DNA helix axis) in the moderately stacked form.

Key words: binding mode, circular and linear dichroism, DNA, poly[d(A-T)$_2$], porphyrin.

Interaction between porphyrins and DNA has been an interesting subject since *meso*-tetra(*p*-*N*-trimethylanilinium)porphyrin (*1*) and tetrakis(3-*N*-methylpyridiniumyl) porphyrin (*2*) were found to form a complex with DNA and poly[d(A-T)$_2$], respectively. The three binding modes for the porphyrin-DNA complexes have been generally accepted (*3–5*, for review), namely, intercalation, outside self-stacking and outside random binding. The groove binding mode was also suggested, mainly by circular and linear dichroism (CD and LD) study (*6–10*).

Self-assembly of drugs is an important phenomenon in biological systems. For porphyrin, self-assembly or aggregation of porphyrin on the DNA template was indicated almost from the outset (*1*, *2*). These porphyrin species that were characterized by a bisignate excitonic induced CD were assigned later to a moderate stacking mode (or modest aggregation). From the studies performed in this direction by Marzilli and his co-workers (*11*, and reference therein) and Pasternack and his co-workers (*12, and reference therein*), the porphyrin species was found to be extensively stacked (or extendedly assembled), and the porphyrins were electronically coupled along the DNA template. The extent of self-aggregation of porphyrin on the DNA template depends on the nature of the central metal ion, the properties of the substituent groups on the periphery of the porphyrin, salt concentration and the template composition of DNA (*2*, *11–20*). An extensively self-stacked form is favored at a high [porphyrin]/[DNA] ratio and at a high salt concentrations, while porphyrin stacks moderately at a low [porphyrin]/[DNA] ratio and at a low salt concentration (*14*, *15*). It was also reported that the shape of bisignate induced CD of self-assembled porphyrin depended on the order of the base-sequence: the CD spectra of the *p*-TMPyP complexes formed with non-alternating homopolymer are characterized by a positive band at short wavelengths followed by a negative band at long wavelengths. In contrast, those complexed with alternating polynucleotide were the opposite to those of non-alternating homopolymers (*21*).

We have been investigating the binding mode of the porphyrin-DNA complex at low porphyrin-to-DNA ratios at which the binding mode of some porphyrin to DNA is expected to be homogeneous and characterizable without interference of the self-assembly of porphyrin (*7*, *10*, *21*, *22*). In the course of our study, we found that *meso*-tetrakis(3-*N*-methylpyridiniumyl)porphyrin (referred to as *m*-TMPyP in this article; Fig. 1) forms a complex with poly[d(A-T)$_2$] at a low porphyrin–DNA ratio and at low NaCl concentrations, resulting in an anomalous bisignate CD spectrum in the Soret band: the magnitude of CD spectrum is about one fold higher than that of monomeric porphyrins (*21*). At similar mixing ratios and salt concentrations, none of the other combinations of related porphyrins, namely, *meso*-tetrakis(*n*-*N*-methylpyridiniumyl)porphyrin (where *n* = 2, 4, referred to as *o*-and *p*-TMPyP, respectively. Fig. 1) and polynucleotide, exhibits this kind of CD spectrum. In this work, we attempt to characterize this anomalous porphyrin species by various spectroscopic methods, including normal absorption, CD and LD.

[*]To whom correspondence should be addressed. Tel: +82-53-810-2362, Fax: +82-53-815-5412, E-mail: seogkim@yu.ac.kr

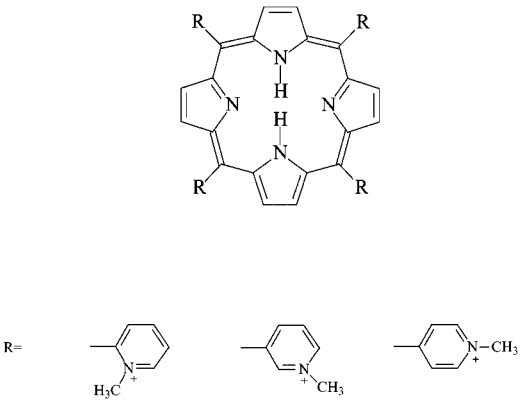

Fig. 1. **Molecular structures of *meso*-tetrakis(*n*-*N*-methylpyridiniumyl)porphyrin (where *n* = 2, 3, and 4, respectively referred to as *o*-, *m*-, and *p*-TMPyP).**

EXPERIMENT

Materials—Porphyrins were purchased from MidCentury (Chicago, IL) and other chemicals from Sigma (Seoul, Korea) and used without further purification. The extinction coefficients of $\varepsilon_{413\ nm}$ = 2.39 × 10^5 cm^{-1} M^{-1}, $\varepsilon_{417\ nm}$ = 2.78 × 10^5 cm^{-1} M^{-1}, and $\varepsilon_{421\ nm}$ = 2.45 × 10^5 cm^{-1} M^{-1} in 5 mM cacodylate buffer at pH 7.0, respectively, were used to determine the concentration of the *o*-, *m*-, and *p*-TMPyP. Synthetic polynucleotides were purchased from Pharmacia (Seoul, Korea) and DNA from Sigma and purified by the method described elsewhere (*22*). The DNA concentrations were determined using molar extinction coefficients of $\varepsilon_{262\ nm}$ = 6,600 cm^{-1} M^{-1}, $\varepsilon_{254\ nm}$ = 8,400 cm^{-1} M^{-1}, $\varepsilon_{251\ nm}$ = 6,900 cm^{-1} M^{-1} and $\varepsilon_{258\ nm}$ = 6,700 cm^{-1} M^{-1} for poly[d(A-T)$_2$], poly[d(G-C)$_2$], poly[d(I-C)$_2$], and calf thymus DNA (referred to as DNA in this work), respectively. The DNA concentrations given in this work thus indicate the concentration of the nucleo-bases. The mixing ratio, *R*, is defined by the ratio [porphyrin]/[nucleo-base]. Samples with various *R* ratios were prepared by adding aliquots of concentrated porphyrin solution (200 μM) to DNA solution (typically 10–20 μl porphyrin solution to 2 ml DNA solution) and the appropriate volume corrections were made. Since the binding mode is affected by ionic strength and the porphyrin–DNA mixing ratio as well as the stacking of porphyrin itself in aqueous solution (*20*), extreme caution was taken with regard to the order of mixing and the concentration of porphyrin stock solution. All measurements were performed at room temperature.

Absorption, CD and LD—The absorption spectra of porphyrins complexed with poly[d(A-T)$_2$] were recorded on a Jasco V550 or Cary 100, and CD spectra on a J-715 spectropolarimeter, displaying the CD in milidegree ellipticity. The path length of cuvettes was 10 mm for both absorption and CD measurements.

Division of measured LD, which is defined by the difference between the parallel and perpendicular components of absorbance relative to the linearly polarized incident light by isotropic absorption, results in a reduced linear dichroism (LD^r). From the magnitude of the LD^r spectrum, the angle between the electric transition moments of the DNA-bound drug and the local DNA helix axis can be calculated (*23–26*). LD spectra were recorded on a Jasco J-500C spectropolarimeter on the flow-aligned porphyrin-DNA complex as described by Nordén and his co-workers.

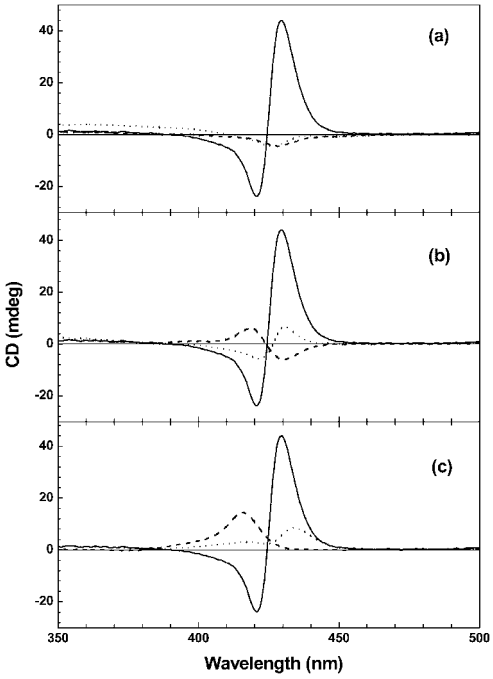

Fig. 2. **(a) Induced CD spectra of *m*-TMPyP complexed with poly[d(A-T)$_2$] (solid curve), poly[d(G-C)$_2$] (dotted curve), and DNA (dashed curve). That of the *m*-TMPyP-poly[d(A-T)$_2$] complex recorded immediately after mixing (b).** Induced CD spectra of *m*-TMPyP complexed with poly[d(A-T)$_2$] (solid curve), poly[d(I-C)$_2$] (dotted curve), and poly(dA)·poly(dT) (dashed curve) and (c) that of the *o*- (dashed curve) and *p*-TMPyP (dotted curve). See text for abbreviations. For all measurements, [TMPyP] = 5 μM, [DNA] = 100 μM in base.

RESULTS

Abnormality of CD Spectrum of the m-TMPyP-Poly[d(A-T)$_2$] Complex Immediately Following Mixing—The excitonic CD spectrum of the *m*-TMPyP-poly[d(A-T)$_2$] complex is compared with those of various porphyrin-polynucleotide complexes in Fig. 2 in order to show its abnormality. In Fig. 2a, the CD spectrum was recorded immediately after *m*-TMPyP had been mixed with poly[d(A-T)$_2$] at a low mixing ratio (*R* = 0.05) and compared with those of *m*-TMPyP complexed with poly[d(G-C)$_2$] and natural DNA under the same *R* ratio and salt concentration. The bisignate CD spectrum (with its negative maximum at 421 nm and positive at 429 nm) of the *m*-TMPyP-poly[d(A-T)$_2$] complex is unique in that the magnitude is at least one order larger than the negative CD band of the *m*-TMPyP-poly[d(G-C)$_2$] and the *m*-TMPyP-DNA complex. The weak negative CD band, which was observed for the *m*-TMPyP when complexed with poly[d(G-C)$_2$] and DNA, indicates that the porphyrin molecule is intercalated between the base pairs of these polynucleotides (*22*).

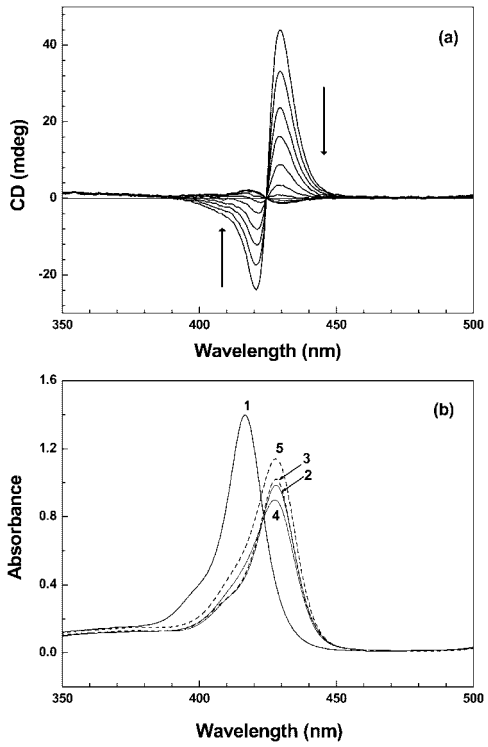

Fig. 3. **(a) Changes in CD spectrum of the *m*-TMPyP-poly[d(A-T)$_2$] complex with time.** In the direction of the arrows, CD was recorded at 0, 20, 40, 60, 90, 120, 150, 180, 210, and 240 min after mixing. **(b) Absorption spectrum of the *m*-TMPyP-poly[d(A-T)$_2$] complex immediately and 24 h after mixing at two representative [TMPyP]/[DNA base] ratios.** Absorption spectrum of the polynucleotide-free *m*-TMPyP (curve 1, thick solid curve) is compared with initial (thin solid curves, curves 2 and 4) and final (24 h after mixing; dashed curves, curves 3 and 5) absorption spectrum of the *m*-TMPyP-poly[d(A-T)$_2$] complex at R = 0.05 (curves 2 and 3) and R = 0.30 (curves 4 and 5). For both (a) and (b) the concentration of TMPyP is 5 μM and that of DNA is 100 μM.

In Fig. 2b, the CD spectrum of the *m*-TMPyP-poly[d(A-T)$_2$] complex is compared with those of the complexes with poly(dA)·poly(dT) and poly[d(I-C)$_2$]. A bisignate CD spectrum for all three complexes is apparent, indicating that porphyrins are stacked along the polynucleotide stem. However, the magnitude again is about five times larger for the *m*-TMPyP-poly[d(A-T)$_2$] complex. The shape of the CD spectrum of the *m*-TMPyP-poly[d(A-T)$_2$] complex immediately after mixing is almost the same as that of the *m*-TMPyP-poly[d(I-C)$_2$] complex (disregarding the intensities), while it is antisymmetric to that of the *m*-TMPyP-poly(dA)·poly(dT) complex. Similar antisymmetric excitonic CD was reported when *p*-TMPyP was complexed with poly[d(A-T)$_2$] and poly(dA)·poly(dT)(*21*). However, the sign of the bisignate CD bands of the *m*-TMPyP-poly[d(A-T)$_2$] complex converted and became similar to that of the *m*-TMPyP-poly(dA)·poly(dT) complex 4 h after mixing (see below for time-dependent CD change, Fig. 3a).

Finally, the initial CD spectrum of the *m*-TMPyP-poly[d(A-T)$_2$] complex is compared to those of the *o*-TMPyP-poly[d(A-T)$_2$] and *p*-TMPyP-poly[d(A-T)$_2$] complexes (Fig. 2c). In contrast with the *m*-TMPyP-poly[d(A-T)$_2$], the *o*-TMPyP-poly[d(A-T)$_2$] complex exhibits a positive CD band, and the *p*-TMPyP-poly[d(A-T)$_2$] complex exhibits two positive bands. From the change in CD spectrum in the presence of a minor groove-binding drug, 4′,6-diamidino-2-phenylindole (referred to as DAPI in this work), and other spectroscopic properties, *o*-TMPyP was suggested to bind at the major groove, while *p*-TMPyP binds near the minor groove and/or the major groove of poly[d(A-T)$_2$] (*22*).

Initial and Final Excitonic CD Spectrum and Other Spectral Properties of the m-TMPyP-Poly[d(A-T)$_2$] Complex at a Low Binding Ratio—The changes in intensity and shape of the excitonic CD spectrum of the *m*-TMPyP-poly[d(A-T)$_2$] complex at R = 0.05 with respect to time is depicted in Fig. 3a. About 1 h after mixing, the intensity of the excitonic CD spectrum decreases by about one order of magnitude and is now comparable with that of the *m*-TMPyP-poly(dA)·poly(dT) and -poly[d(I-C)$_2$] complexes. The sign is reversed: An initial negative CD band at 421 nm and positive band at 429 nm immediately after mixing converted to a positive band at 418 nm and a negative band at 430 nm. The shape of the final stabilized CD spectrum of the *m*-TMPyP-poly[d(A-T)$_2$] complex is similar to that of the *m*-TMPyP-poly(dA)·poly(dT) complex, which is in contrast to the fact that the excitonic CD of the *p*-TMPyP-poly(dA)·poly(dT) complex is oppsite in sign compared to the *p*-TMPyP-poly[d(A-T)$_2$](*10*, *22*). The time-dependent CD spectrum exhibits an isosbestic wavelength at 424 nm, suggesting that the change in CD spectrum occurs between two states which are represented by a strong excitonic CD with negative and positive bands (from short wavelength) and a weak excitonic CD with its order of positive and negative bands reversed.

The absorption spectra of the *m*-TMPyP-poly[d(A-T)$_2$] complex immediately after mixing and that at 24 h after mixing at the mixing ratios of 0.05 and 0.3, as well as polynucleotide-free *m*-TMPyP, are compared in Fig. 3b. Polynucleotide-free porphyrin exhibited a strong absorption band at 417 nm with a shoulder at about 400 nm, which remained unchanged with time (curve 1). In the presence of poly[d(A-T)$_2$] at a low mixing ratio (R = 0.05), a red-shift of 11 nm and ~29% hypochromism were apparent immediately after mixing. This moderate change in the absorption spectrum, which is typical of porphyrin that binds outside of DNA, is in contrast to the absorption spectra of the same porphyrin in the presence of poly[d(G-C)$_2$] or DNA (16–17 nm red shift and 50–55% hypochromism, data not shown). The overall shape and intensity of the absorption spectrum was retained for the *m*-TMPyP-poly[d(A-T)$_2$] complex at this low mixing ratio, although a small increase in absorbance was apparent 24 h after following mixing (curves 2 and 3 in Fig. 3b). At a higher mixing ratio (R = 0.30), hypochromism is more pronounced than at a low mixing ratio (~36%, curve 4 in Fig. 3b). After 24 h, an increase in absorbance without band shift (~27% hyperchromism compared to initial complex) was apparent (curve 5 in Fig. 3b). Although it was not exactly the same, the tendency of the change in absorption spectra was similar at a mixing ratio higher than 0.25 (data not shown).

LD of the *m*-TMPyP-poly[d(A-T)$_2$] and *p*-TMPyP-poly[d(A-T)$_2$] complex immediately after mixing and 3 h after mixing are compared in Figs. 4, a and b, respectively. A small negative LD signal in the Soret band (425

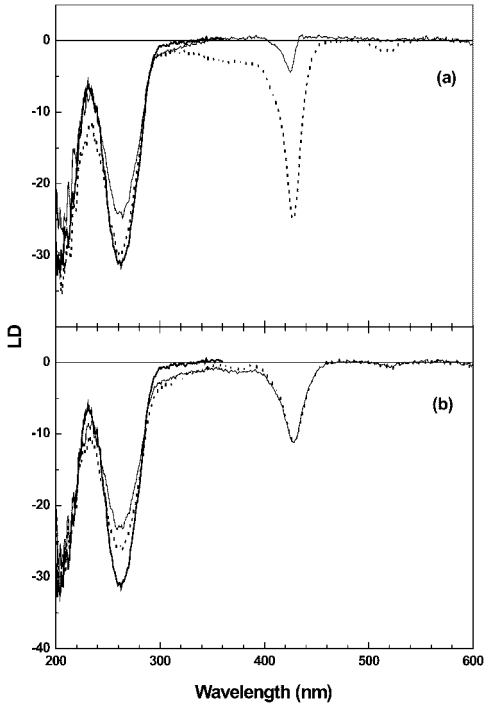

Fig. 4. **LD spectra of the *m*-TMPyP (a) and *p*-TMPyP (b) complexed with poly[d(A-T)$_2$] immediately (solid curves) and 3 h after (dotted curves) mixing.** LD spectrum of porphyrin-free polynucleotide is compared as thick curve. The conditions and concentration are the same as in Fig. 3.

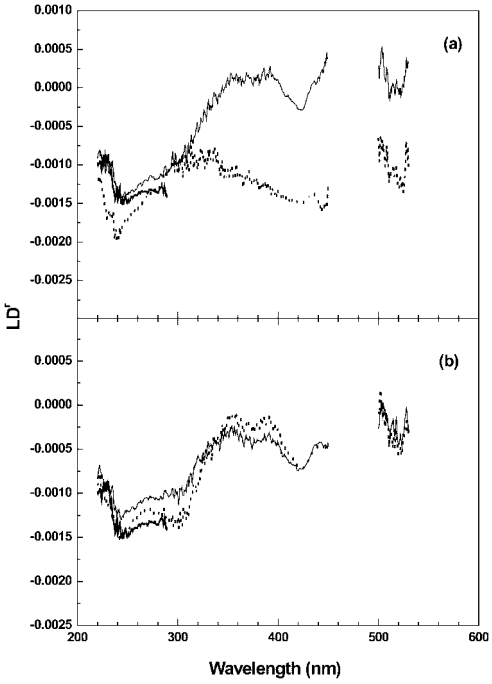

Fig. 5. **Reduced LD calculated by division of measure LD by isotropic absorption.** Conditions and the curve assignment are the same as in Fig. 4.

nm) of the *m*-TMPyP-poly[d(A-T)$_2$] was apparent immediately after mixing. The magnitude of this initial band increased, and the maximum shifted 2 nm towards longer wavelength at 1 h after mixing. In the DNA absorption region (near 260 nm), the magnitude of LD decreased upon adding both porphyrins, suggesting that the helical structure of DNA near the porphyrin binding site is either partially dissociated or bent immediately after mixing. With time, the LD magnitude of the *m*-TMPyP-poly[d(A-T)$_2$] complex in the DNA absorption region was restored to that of porphyrin-free poly[d(A-T)$_2$] (Fig. 4a). In contrast, the LD magnitude tended to recover, but this recovery was not complete in the case of *p*-TMPyP-poly[d(A-T)$_2$] complex. The magnitude of LD in the Soret region of the *p*-TMPyP-poly[d(A-T)$_2$] complex is between the initial and final magnitudes of the *m*-TMPyP-poly[d(A-T)$_2$] complex. The measured LD spectrum is divided by the isotropic absorption spectrum to give an LD^r spectrum from which the angle β between degenerated electronic transition and the local DNA helix axis can be calculated (*27*).

This property makes LD^r very useful to determine the binding mode of the drug relative to the polynucleotide (*25*) and was applied to some of the porphyrin-DNA complexes (*7*, *10*, *20–22*, *28*). The angles of both the B_x and B_y transitions of *m*-TMPyP relative to the local poly[d(A-T)$_2$] helix axis were calculated from the maximum and minimum values (Fig. 5a). Initially, these angles are 41–44°, which coincides with the angle between the transition moments of the minor groove-binding drugs such as Hoechst 33258 and DAPI and the DNA local helix axis (*29*, *30*). As time passes, this angle becomes larger and stabilized at the angle of 84–86°. Considering that the angle of the DNA base relative to the local helix axis was assumed to be 86° for the LD^r calculation, the molecular plane of porphyrin in the final stabilized complex is almost parallel to the DNA bases (perpendicular to the helix axis). On the other hand, no significant change between the initial and final LD^r spectrum (which corresponds to 53–60° between the in-plane transition dipole and the DNA helix axis) was observed for the *p*-TMPyP-poly[d(A-T)$_2$] complex (Fig. 5b) as was reported earlier (*22*). It was recently reported that the LD^r spectrum of the porphyrin-DNA complex is sensitive to the condition of the complex including the salt concentration and the mixing ratio (*20*). Therefore, the salt concentration and the mixing ratio were kept constant throughout this work (5 mM Na^+ from buffering cacodylate molecule, no salt was added, and R = 0.05).

Mixing Ratio and Time Dependence of the Excitonic CD of the m-TMPyP-poly[d(A-T)$_2$] Complex—Figure 6a shows the time-dependent change in CD intensity at 430 nm for the *m*-TMPyP-poly[d(A-T)$_2$] complex and LD at 427 nm at a low mixing ratio (R = 0.05). The initial and final CD intensities (24 h after mixing) at 430 nm at various mixing ratios are depicted in Fig. 3b. A large and relatively fast decrease in CD intensity at 430 nm is observed at this low mixing ratio: Decrease in CD intensity was achieved in about two 2.5 h. The shape of the final CD spectrum is reversed from that of the initial one as was discussed in detail in the previous section. The change in CD is slower at mixing ratios of 0.10 and 0.15: The reaction is complete in 5–7 h at R = 0.1 (data not shown). The shape of bisignate CD was never reversed at these mix-

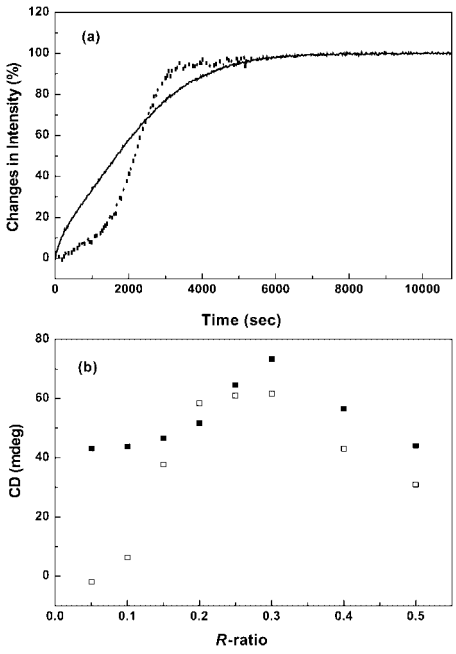

Fig. 6. **(a) Changes in CD (solid curve) intensity at 430 nm of the *m*-TMPyP-poly[d(A-T)$_2$] complex and that of LD (dotted curve) at 417 nm with time.** For both measurements, [*m*-TMPyP] = 5 μM and R = 0.05 and (b) initial (closed squares) and final (24 h after mixing; open squares) CD intensity at 430 nm at various mixing ratios.

ing ratios, which is in contrast to that at R = 0.05. Contrarily, at the mixing ratio of 0.20, the CD intensity at 430 nm tends to increase. Therefore, as the mixing ratio corresponds to one porphyrin molecule per 5–6 DNA bases or 2.5–3.0 base pairs, changes in the porphyrin binding mode result in an increase in CD intensity. As the mixing ratio is further increased, both the intensity at 420 nm of the negative peak and at 430 nm of the positive peak decrease again, but this decrease is very slow compared to that at low mixing ratios. Here, the shape of the final CD spectrum is exactly the same as its initial form. In contrast with CD intensity, the change in magnitude of LD at 427 nm exhibits a sigmoidal curve: The increase in LD intensity is very slow until 30 min later, when a relatively rapid change follows. It should be noted that excitonic CD reflects the coupling of the electric dipole moment between the porphyrin molecules, while LD measures the angle between the polynucleotide helix axis and the electric dipole moment (see below). At higher mixing ratios ($R \geq 0.20$), the LD signal collapsed, probably due to the aggregation of DNA itself (data not shown).

DISCUSSION

Initial and Final Assemblies of m-TMPyP to poly[d(A-T)$_2$] at Various Binding Ratios—The aggregation of various porphyrins on DNA templates have been extensively studied since the first report of such aggregation (*1*). In particular, the stacking of *meso*-tetrakis[4-[(3-(trimethylammonio)propyl)-oxy]phenyl]porphyrin (TθOPP) (*14*, *15*, *31*) on various DNA molecules under various conditions has been systematically studied. Extensively self-stacked TθOPP, which favors high mixing ratios and high salt concentrations, is characterized by a relatively low-intensity conservative CD and a large hypochromicity in the Soret band of the absorption spectrum. In contrast, moderately stacked TθOPP favors low mixing ratios and low salt concentrations: the CD signal is more intense and the hypochromicity is less pronounced for moderately stacked TθOPP. On the other hand, Pasternack and his co-workers observed a bisignate, non-symmetric spectrum, with a magnitude one to two orders larger than those of the monomerically bound porphyrins for DNA-bound *trans*-bis(*N*-methylpyridiniumyl)diphenylporphyrin and its Cu(II) complex (*12*, *13*, *17*). The shape and intensity of the CD signal was best accounted for as the result of the electric field produced by a coupling of one oscillating dipole with the other dipoles in the organized array of porphyrin molecules (*18*).

Considering that (1) the magnitude of excitonic CD is in a comparable range to those reported by Pasternack and his co-workers, and (2) the excitonic CD disappears at low mixing ratios but remains at higher mixing ratios, the initial intense bisignate CD spectrum in the Soret band of the *m*-TMPyP-poly[d(A-T)$_2$] complex can conceivably be understood as an extensive (stacked) aggregation of the porphyrin molecules. However, the final less intense reversed CD spectrum is a moderately stacked form (at R = 0.05), although the intensity of excitonic CD is the opposite of those reported by Marzilli and his coworkers. This discordance may be accounted for by the difference in porphyrins and the particularity of *m*-TMPyP. The change in magnitude and the shape of the final CD spectrum is more pronounced for the lower mixing ratios of below 0.2: the change is the most significant for R = 0.05 and least for R = 0.15. This result probably reflects a situation in which the *m*-TMPyP molecules concentrate initially at the local regions of the poly[d(A-T)$_2$] template to form an extensive assembly, and from there they start to disperse to result in a moderately-stacked array. At high mixing ratios, this dispersion may be prevented by crowded *m*-TMPyP. We did not find any evidence of self-stacking of *m*-TMPyP in aqueous solution in the absence of polynucleotide up to 1 M salt concentration: the absorption spectrum was identical at 0 M and 1 M NaCl, and also identical within the concentrations adopted in this work (data not shown). Therefore, self-stacking of porphyrin prior to polynucleotide binding is not an important factor for observed excitonic CD spectra in the case of *m*-TMPyP.

Electron richness or deficiency of the side chain on the periphery phenyl or pyridinium ring has been suspected to be the reason for the formation of stacked array porphyrins and has been systematically investigated by Marzilli and his co-workers (*11*, *14–16*). However, the two locations of *p*- and *m*-TMPyP seem too close to be considered as a different tentacle. Rather, the difference in distance between the two positive charges of the *N*-methyl group may account for this difference in binding mode. Since the only difference between the *m*- and *p*-TMPyP is the location of the positive charge (distance between the charges), the electrostatic interaction between the phosphate groups of the polynucleotide and the porphyrin molecules of *p*-TMPyP may prevent the self-assembly of the porphyrins at a very low mixing ratio. In other words,

the distance between the two positive charges of the pyridinium ring at opposite sides of the *p*-TMPyP molecules coincides with that between phosphate groups, while the distance between the positive charges is, on average, short and variable in *m*-TMPyP and may conceivably result in porphyrin-porphyrin assembly at a low mixing ratio.

It is noteworthy that the magnitude of LD at 260 nm, which reflects the orientability of DNA, initially decreased when *m*-TMPyP was mixed with poly[d(A-T)$_2$] and was restored over time. This observation indicates that an extensive aggregation of porphyrin results in a bend of the DNA template. Further increase in porphyrin concentration results in a collapsed LD (data not shown), implying the aggregation of DNA itself. As the porphyrin dispersed to a moderately stacked form, the orientation of DNA recovered, indicating that the moderately stacked porphyrins do not interfere with the DNA conformation.

Uniqueness of the m-TMPyP-poly[d(A-T)$_2$] Complex—The weak negative CD band (Fig. 2a) indicated that *m*-TMPyP intercalates between the base pairs of poly[d(G-C)$_2$] and DNA. On the other hand, the uniquely large bisignate CD of the *m*-TMPyP-poly[d(A-T)$_2$] complex indicated an extensive aggregation of *m*-TMPyP on the poly[d(A-T)$_2$] template, which is unstable at a low mixing ratio. In the *p*-TMPyP-poly[d(G-C)$_2$] and *p*-TMPyP-poly[d(I-C)$_2$] complexes, the spectral properties were similar at a low mixing ratio (R = 0.05) and low salt concentration, and both can be accounted as an intercalation (*32*). As the mixing ratio and/or salt concentration increased, the absorption and CD spectra of the *p*-TMPyP-poly[d(I-C)$_2$] complex began to resemble those of the *p*-TMPyP-poly[d(A-T)$_2$] complex, indicating that the amine group that protrudes in the minor groove contributes, at least in part, in stabilizing the intercalated porphyrins. Lack of the amine group in the minor groove may be part of the reason for the preference of outside binding for *m*-TMPyP to poly[d(A-T)$_2$].

At a low mixing ratio (R = 0.05), both *o*-TMPyP and *p*-TMPyP exhibited positive induced CD band(s) in the Soret absorption region when complexed with poly[d(A-T)$_2$], in sharp contrast to the case of *m*-TMPyP (Fig. 2c). The *o*-TMPyP, at which the periphery pyridinium ring is restricted from free-rotation, was concluded to sit in the major groove, where the molecular plane of porphyrin is probably almost parallel to the flat surface of the major groove. In contrast, *p*-TMPyP binds either at the outside of the minor groove (not edgewise insertion) or at the major groove or both binding modes co-exist (*22*). In the case of *o*-TMPyP, the bulky pyridinium ring may prevent self-stacking of the porphyrin molecules.

In the presence of poly(dA)·poly(dT) and poly[d(I-C)$_2$], *m*-TMPyP exhibited bisignate CD spectra in the Soret band, indicating self-association of porphyrin on both the polynucleotide templates (Fig. 2b). The CD spectrum appeared to be antisymmetric. It was reported that the sign of the excitonic CD spectrum of *p*-TMPyP, which was observed at high mixing ratios, was the opposite in a complex with a non-alternating homopolymer compared with those in complexes with alternating polynucleotides, disregarding the nature of the base pair (*22*). Although the reason for dependence of the sign of the excitonic CD on the polynucleotide remains to be investigated, *m*-TMPyP complexed with poly(dA)·poly(dT) and poly[d(I-C)$_2$] is another example of the dependence of the order of positive and negative CD in the Soret absorption band on the base arrangement. As can be judged by the magnitude, *m*-TMPyP extensively aggregates initially on the poly[d(A-T)$_2$] (Fig. 2b). The order of positive and negative CD is the same as in the case of poly[d(I-C)$_2$], that is, the positive at long wavelength and the negative at short wavelength. The shape of excitonic CD of extensively aggregated *m*-TMPyP might be related to the structure of the minor groove, since that of poly[d(A-T)$_2$] resembles poly[d(I-C)$_2$]. However, the sign of the final excitonic CD for the *m*-TMPyP-poly[d(A-T)$_2$] complex is the opposite of that of the initial mixture (Fig. 3a). The reason for this exception is under investigation in our laboratory.

Initial and Final Binding Geometry of m-TMPyP to poly[d(A-T)$_2$]—The angles of both the B_x and B_y in-plane transition dipoles of porphyrin with respect to the polynucleotide helix are in the range of 53–60° for the *p*-TMPyP-poly[d(A-T)$_2$] complex (Fig. 5b). These angles, together with the monomeric positive CD spectrum, indicated that *p*-TMPyP locates either at the major groove, or near the minor groove, or at both binding sites (*22*). In the *m*-TMPyP-poly[d(A-T)$_2$] complex, the angle was reported to be 61–74° in the same article. However, from analysis of the initial and final LD^r by taking into account that the LD signal is time-dependent, the initial angle between the porphyrin molecular plane and the poly[d(A-T)$_2$] helix axis was 41–44°, and the final value corresponds to an angle of 84–86°. Therefore, the angle previously reported as 61–74° may reflect a state between the initial and final form of the *m*-TMPyP-poly[d(A-T)$_2$] complex. Although the initial angle of 41–44° is close to that of drugs that bind along the minor groove, it cannot be described by the minor groove binding model because the self-associated porphyrin cannot be cramped in the narrow minor groove. It is clear that the molecular plane of the porphyrin molecule is not parallel to the DNA bases (not perpendicular to the DNA helix axis) in the extensively "stacked" assembly. Stacked porphyrins in this model may tilt strongly from the DNA base plane. In the moderately aggregated form, porphyrin forms an array of stacked assembly and its molecular plane is perpendicular to the DNA helix axis.

This work was supported by Korea Science and Engineering Foundation (Grant no.: R01–2000–000–00043–0).

REFERENCES

1. Carvlin, M.J., Datta-Gupta, N., and Fiel, R.J. (1982) Circular dichroism spectroscopy of a cationic porphyrin bound to DNA. *Biochem. Biophys. Res. Commun.* **108**, 66–73
2. Pasternack, R.F., Gibbs, E.J., and Villafranca, J.J. (1983) Interactions of porphyrins with nucleic acids. *Biochemistry* **22**, 2406–2414
3. Fiel, R.J. (1989) Porphyrin-nucleic acid interactions: A review. *J. Biomol. Struct. Dyn.* **6**, 1259–1274
4. Marzilli, L.G. (1990) Medical aspects of DNA-porphyrin interactions. *New J. Chem.* **14**, 409–420
5. Pasternack, R.F. and Gibbs. E.J. (1996) Porphyrin and metalloporphyrin interactions with nucleic acids in *Metal Ions in Biological Systems* (Sigel, H., ed.) Vol. **33**, pp. 367–377, Marcel Dekker, New York

6. Kuroda, R. and Tanaka, H. (1994) DNA-porphyrin interactions probed by induced CD spectroscopy. *J. Chem. Soc. Chem. Commun.* 1575–1576
7. Sehlstedt, U., Kim, S.K., Carter, P., Goodisman, J., Vollano, J.F., Nordén, B., and Dabrowiak, J.C. (1994) Interaction of cationic porphyrins with DNA. *Biochemistry* **33**, 417–426
8. Schneider, H.-J. and Wang, M. (1994) DNA interactions with porphyrins bearing ammonium side chains. *J. Org. Chem.* **59**, 7473–7478
9. Lipcomb, L.A., Zhou, F.X., Presnell, S.R., Woo, R.J., Peek, M.E., Plaskon, R.R., and Williams, L.D. (1996) Structure of a DNA-porphyrin complex. *Biochemistry* **35**, 2818–2823
10. Yun, B.H., Jeon, S.H., Cho, T.-S., Yi, S.Y., Sehlstedt, U., and Kim, S.K. (1998) Binding mode of porphyrins to poly[d(A-T)$_2$] and poly[d(G-C)$_2$]. *Biophys. Chem.* **70**, 1–10
11. Trommel, J.S. and Marzilli, L.G. (2001) Synthesis and DNA binding of novel water-soluble cationic methylcobalt porphyrins. *Inorg. Chem.* **40**, 4374–4383
12. Pasternack, R.F., Ewen, S., Rao, A., Meyer, A.S., Freedman, M.A., Collings, P.J., Frey, S.L., Ranen, M.C., and de Paula, J.C. (2001) Interaction of copper(II) porphyrins with DNA. *Inorg. Chim. Acta* **317**, 59–71
13. Gibbs, E.J., Tinoco Jr. I., Maestre, M.F., Ellinas, P.A., and Pasternack, R.F. (1988) Self-assembly of porphyrins on nucleic acid templates. *Biochem. Biophys. Res. Commun.* **157**, 350–358
14. Mukundan, N.E., Pethö, G., Dixon, D.W., Kim, M.S., and Marzilli, L.G. (1994) Interaction of an electron-rich tetracationic porphyrin with calf thymus DNA. *Inorg. Chem.* **33**, 4676–4687
15. Mukundan, N.E., Pethö, G., Dixon, D.W., and Marzilli, L.G. (1995) DNA-tentacle porphyrin interactions: AT over GC selectivity exhibited by an outside binding self-stacking porphyrin. *Inorg. Chem.* **34**, 3677–3687
16. McClure, J.E., Baudouin, L., Mansuy, D., and Marzilli, L.G. (1997) Interactions of DNA with a new electron-deficient tentacle porphyrin: meso-tetrakis[2, 3, 5, 6-tetrafluoro-4-(2-trimethylammoniumethylamine)phenyl]porphyrin. *Biopolymers* **42**, 203–217
17. Pasternack, R.F., Giannetto, A., Pagano, P., and Gibbs, E.J. (1991) Self-assembly of porphyrin on nucleic acids and polypeptides. *J. Am. Chem. Soc.* **113**, 7799–7800
18. Pasternack, R.F., Bustamante, C., Collings, P.J., Giannetto, E.J., and Gibbs, E.J. (1993) Porphyrin assemblies on DNA as studied by a resonance light-scattering technique. *J. Am. Chem. Soc.* **115**, 5393–5399
19. Pasternack, R.F. and Gibbs, E.J. (1993) Porphyrin Assembly Formation on Helical *Biopolymers*. *J. Inorg. Organomet. Polym.* **3**, 77–88
20. Ismail, M.A., Rodger, P.M., and Rodger, A. (2000) Drug-self-assembly on DNA: Sequence effects with trans-bis-(4-N-methylpyridiniumyl)diphenyl porphyrin and Hoechst 33258. *J. Biomol. Str. Dyn. Conversation* **11**, 335–348
21. Lee, S., Jeon, S.H., Kim, B.-J., Han, S.W., Jang, H.G., and Kim, S.K. (2001) Classification of CD and absorption spectra in the Soret band of H_2TMPyP bound to various synthetic polynucleotides. *Biophys. Chem.* **92**, 35–45
22. Lee, S., Lee, Y.-A., Lee, H.M., Lee, J.Y., Kim, D.H., and Kim. S.K. (2002) Rotation of periphery methylpyridine of meso-tetrakis(n-N-methylpyridiumyl)porphyrin (n=2, 3, 4) and its selective binding to native and synthetic DNAs. *Biophys. J.* **83**, 371–381
23. Nordén, B. and Tjerneld, F. (1976) High-selectivity linear dichroism as a tool for eguilibrium analysis in biochemistry: Stability constant of DNA-ethidium bromide complex. *Biophys. Chem.* **4**, 191–198
24. Nordén, B. and Seth, S. (1985) Critical aspects of measurement of circular and linear dichroism – A device for absolute calibration. *Appl. Spectrosc.* **39**, 647–655
25. Nordén, B., Kubista, M., and Kurucsev. T. (1992) Linear dichroism spectroscopy of nucleic acids. *Q. Rev. Biophys.* **25**, 51–170
26. Nordén, B. and Kurucsev, T. (1994) Analyzing DNA complexes by circular and linear dichroism. *J. Mol. Recognit.* **7**, 141–156
27. Härd, B. and Nordén, B. (1986) Enantioselective interactions of inversion-labile trigonal iron[II] complexes upon binding to DNA. *Biopolymers* **25**, 1209–1228
28. Geacintov, N.E., Ibanez, V., Rougee M., and Bensasson, R.V. (1987) Orientation and linear dichroism characteristics of porphyrin-DNA complexes. *Biochemistry* **26**, 3087–3092
29. Eriksson, S., Kim, S.K., Kubista, M., and Nordén, B. (1993) Binding of 4′, 6-diamidino-2-phenylindole to AT regions of DNA: Evidence for an allosteric conformational change. *Biochemistry* **32**, 2987–2998
30. Moon, J.-H., Kim, S.K., Sehlstedt, U., Rodger, A., and Nordén, B. (1996) DNA structural features responsible for sequence-dependent binding geometries of Hoechst 33258. *Biopolymers* **38**, 593–606
31. Marzilli, L.G., Pethö, G. Lin, M. Kim, M.S., and Dixon. D.W. (1992) Tentacle porphyrins: DNA interactions. *J. Am. Chem. Soc.* **114**, 7575–7577
32. Lee, Y.-A., Lee, S., Cho, T.-S., Kim, C., Han, S.W., and Kim, S.K. (2002) Binding mode of meso-tetrakis(*N*-methylpyridiumyl) porphyrin to poly[d(I-C)$_2$]: Effect of amino group at the minor groove of poly[d(G-C)$_2$] on the porphyrin-DNA interaction. *J. Phys. Chem.* **106**, 11351–11355